Electronic Supplementary Material (ESI) for Physical Chemistry Chemical Physics.

Electronic supplementary information: Photoprotection through triplet energy transfer in higher plants: the role of electronic and nuclear fluctuations

Lorenzo Cupellini, Sandro Jurinovich, Ingrid Guarnetti Prandi, Stefano Caprasecca, and Benedetta Mennucci*

Dipartimento di Chimica e Chimica Industriale, University of Pisa, Via G. Moruzzi 13, 56124 Pisa, Italy

E-mail: benedetta.mennucci@unipi.it

S1 Details on the Molecular Dynamics simulation

We followed the procedure set up by Ogata et al.[1] for the simulation of the entire Photosystem II. Such procedure is evidently sufficient for the simulation of the sole CP29.

The ff99SB force-field[2] has been used for the protein, lipid14[3] for the lipids. The parameters for the cofactors were built as follows: for Chl a were taken from Zhang at al.,[4] and used without modifications. Chl b differs from Chl a only at the C7 position, where the methyl is substituted by a formyl group. The missing parameters for the formyl were taken from the general AMBER force field.[5] The partial charges derived by Zhang are for the AMBER03 family (derived by using B3LYP with TZ basis set with a continuum solvation model). In order to be consistent with the ff99SB and lipid14 force-fields adopted for the protein , we re-derived compatible partial charges from a fitting of the electrostatic potential calculated at the Hartree-Fock 6-31G* level.[2]

The minimization was performed in three steps: firstly, the hydrogen atoms were relaxed, maintaining all the other atoms frozen. Then, the water molecules, the ions, and the lipid molecules were relaxed, with the protein and cofactors frozen. Finally, all the system was minimized. The system was heated from 0K to 100K with a 5 ps NVT simulation, then from 100K to 300K with a 100 ps NPT simulation, as suggested by the for lipid bilayer membrane simulations by the authors of the Amber lipid14 force field.[3] During the heating, weak harmonic constraints (10.0 kcal mol^{-1} $Å^{-1}$) were set for the lipids, as well as for the entire protein and the cofactors. The equilibration of the system was performed with a 6 ns NPT simulation, initially mantaining the previously setup constraints on the protein, the cofactors, and the lipids. In this step the constraint on lipids and complex was released gradually over 5 ns (-1.0 kcal mol^{-1} $Å^{-1}$ every 500 ps) until the force constraint became equal to zero. The last nanosecond of simulation was run without constraint. The production was

performed on an 80 ns NPT simulation. For all simulations, the integration step was set to 1 fs. The temperature and pressure were controlled, respectively, by a Langevin thermostat and the anisotropic barostat implemented in Amber14. The structural parameters of the simulation are shown in Figure S5.

S2 Calculation of the Spectral overlap

The quantity J_{DA} in equation (1) is the so-called spectral overlap, and may be written as:

$$J_{DA} = \int_{-\infty}^{\infty} \mathrm{d}E f_D(E) f_A(E) \tag{S1}$$

where $f_D(E)$ and $f_A(E)$ are the FCWD functions, that may be expressed as a function of the absorption spectrum of A $\varepsilon_A(E)$ and the emission spectrum of D ($f_D(E)$):[6,7]

$$\begin{aligned} f_A(E) &= \frac{\varepsilon_A(E)/E}{\int_{-\infty}^{\infty} \mathrm{d}E \varepsilon_A(E)/E} \\ f_D(E) &= \frac{A_D(E)/E^3}{\int_{-\infty}^{\infty} \mathrm{d}E A_D(E)/E^3} \end{aligned} \tag{S2}$$

Following You and Hsu,[7] we compute the FCWD functions from a fitting of the experimental spectra, and used eq. (S1) to compute the spectral overlap. The absorption and emission spectra were fitted with simple single-mode vibronic expressions:

$$A_D(E) = \sum_m \left(1 - \frac{m\hbar\omega}{E_0}\right)^3 \frac{S^m}{m!} \exp\left(-\frac{(E - E_0 + m\hbar\omega)^2}{2\sigma^2}\right) \tag{S3}$$

$$\varepsilon_A(E) = \sum_m \left(1 + \frac{m\hbar\omega}{E_0}\right) \frac{S^m}{m!} \exp\left(-\frac{(E - E_0 - m\hbar\omega)^2}{2\sigma^2}\right) \tag{S4}$$

The fit parameters E_0 and ω correspond to the 0-0 transition energy and to the vibrational frequency, S is the Huang-Ryhs factor, and σ is the broadening of each vibronic band. We use the full-width at half-maximum, that is fwhm $= 2\sqrt{2\ln 2}\sigma$.

As the triplet spectra of carotenoids are not available in the literature, we fit the parameters ω, S and fwhm to the absorption spectra of the S_2 states of the carotenoids. The energy of carotenoid triplets is often estimated as half of the S_1 energy.[8] There are different estimates for the S_1 energy of Vio and Lut,[9] but in LHCII the two S_1 states are very close in energy, around 14000 cm^{-1}, therefore we used a 0-0 transition energy of 7000 cm^{-1} for both carotenoids, which is consistent with the T_1 energy for other carotenoids with the same conjugation length.[8,10] The parameters for Chl a were fitted directly to the phosphorescence spectrum.[11]

The final parameters are summarized in Table S1. With these parameters, we estimate a spectral overlap of 1.31 eV^{-1} between Chl a and Lutein, and 1.26 eV^{-1} between Chl a and Violaxanthin. We note that an uncertainty of $\pm$ 200 cm^{-1} on the triplet energy of the Cars would imply a variation of $\pm$ 10% on the spectral overlap. The spectral overlap between two Chls is 2.84 eV^{-1}. We also note that variations in the order of 10% on the other parameters result in less than 6% variation on the spectral overlap.

Table S1: Parameters used for the calculation of the spectral overlap as in eqs. S3,S4,S1 and S2. The Huang-Ryhs factor S is dimensionless, the other parameters are in cm^{-1}.

	E_0	S	ω	fwhm
Chlorophyll a	10230	0.5121	1050	705
Lutein	7000	1.227	1453	1318
Violaxanthin	7000	1.203	1382	1094

S3 Delocalization length

As a measure of delocalization, we use the Inverse Participation Ratio (IPR), obtained from the coefficients of the localized states on the adiabatic state of a dimer.

$$\mathrm{IPR} = \left(\sum_{k=1}^{N} C_{ik}^4 \right)^{-1} \tag{S5}$$

Where C_{ik} is the coefficient of the localized state i in the adiabatic state k:

$$|k\rangle = \sum_{i=1}^{N} C_{ik} \, |i\rangle \quad \text{, and} \quad \sum_{i=1}^{N} C_{ik}^2 = 1 \tag{S6}$$

A completely delocalized state has an IPR of N, and a localized state has an IPR of 1.

S4 Figures and Tables

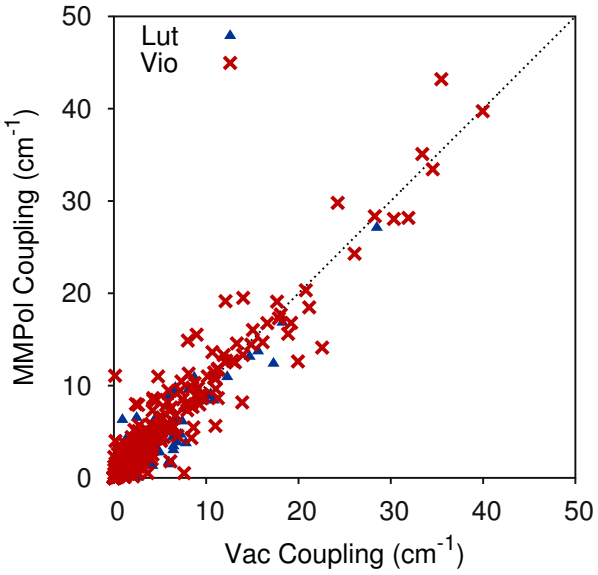

Figure S1: Scatter plot of MMPol absolute couplings versus absolute couplings computed in vacuo. Blue triangles represent the couplings involving Lutein, while red crosses represent coupplings involving Violaxanthin. The $x = y$ line is represented for reference.

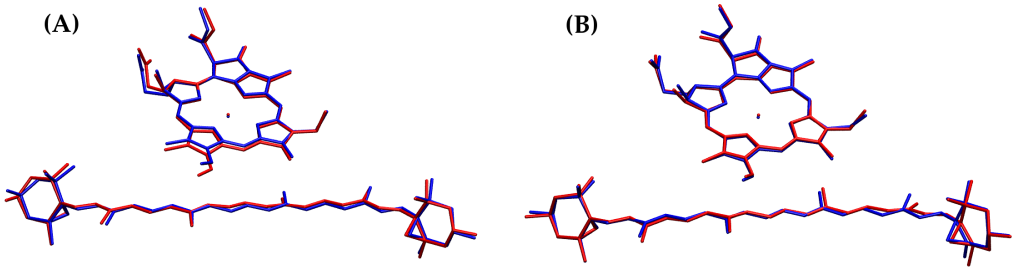

Figure S2: The configurations that give rise to the strongest (A) and weakest (B) couplings (red), superimposed to the same configurations after optimization (blue).

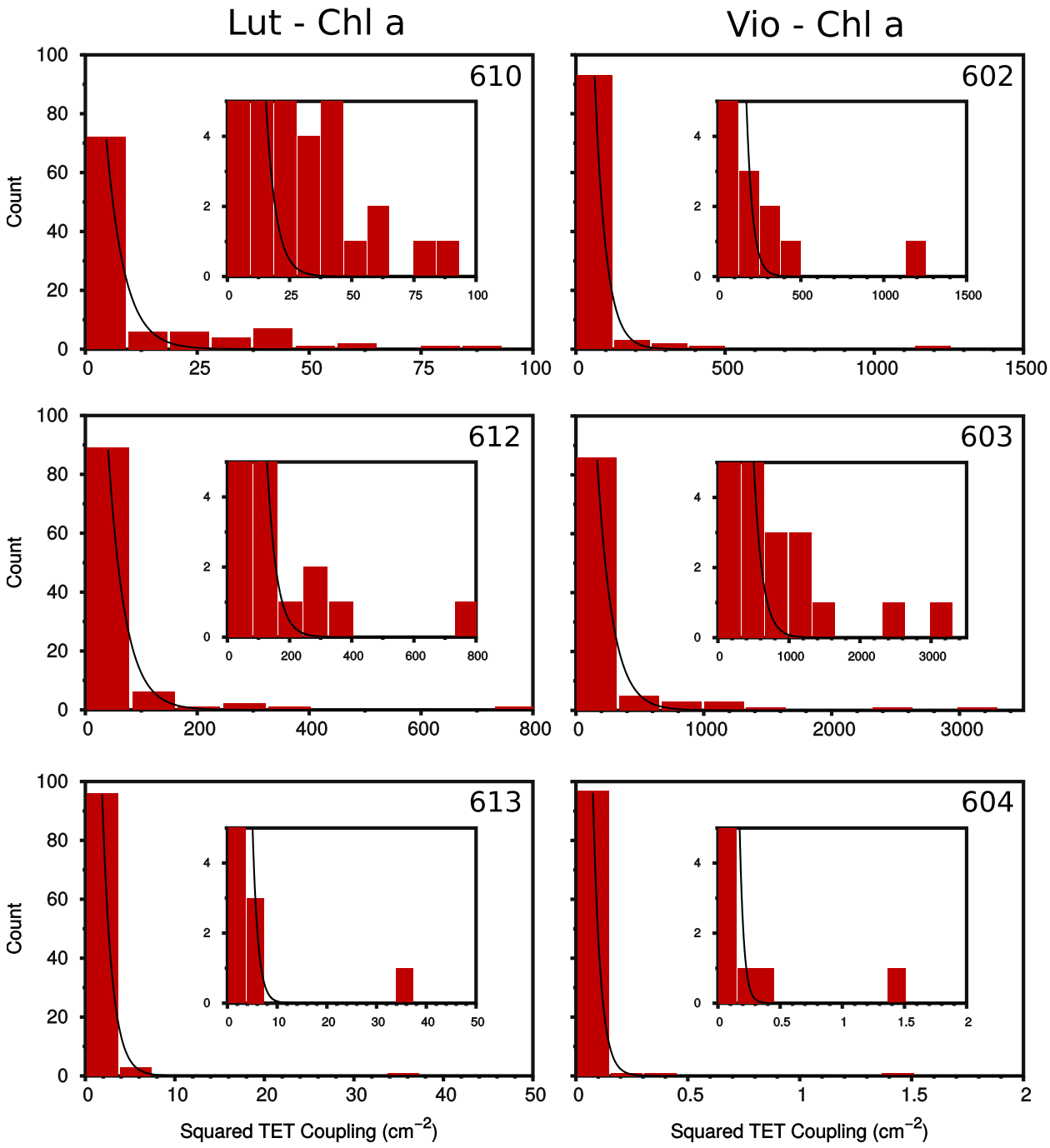

Figure S3: Distribution of squared TET couplings obtained for all Car-Chl pairs. The solid black lines represent an exponential fit.

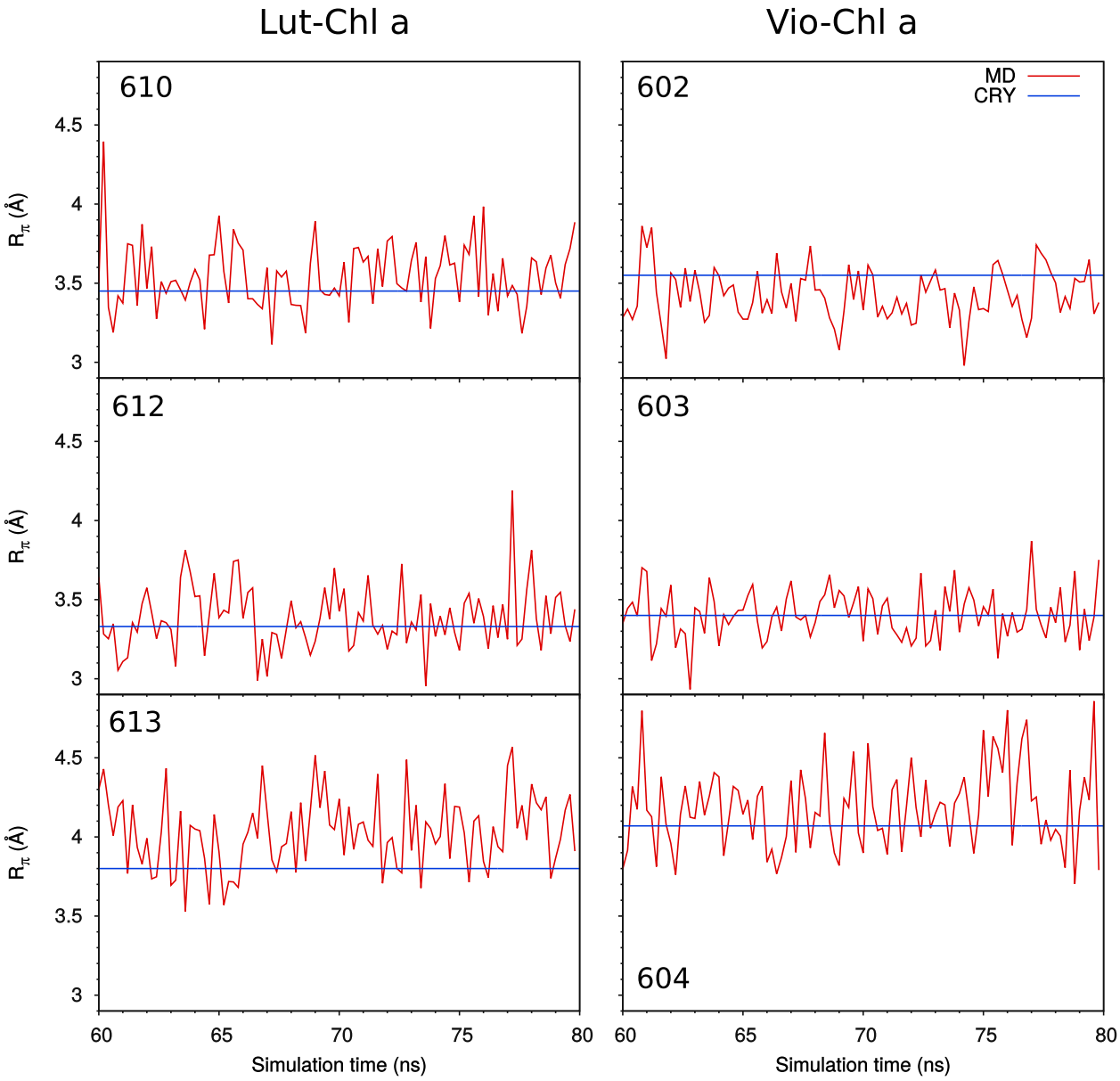

Figure S4: Fluctuation of R_π during the part of the simulation that we used for coupling calculations. R_π is reported for all Car-Chl pairs and compared to the value in the crystal structure (blue).

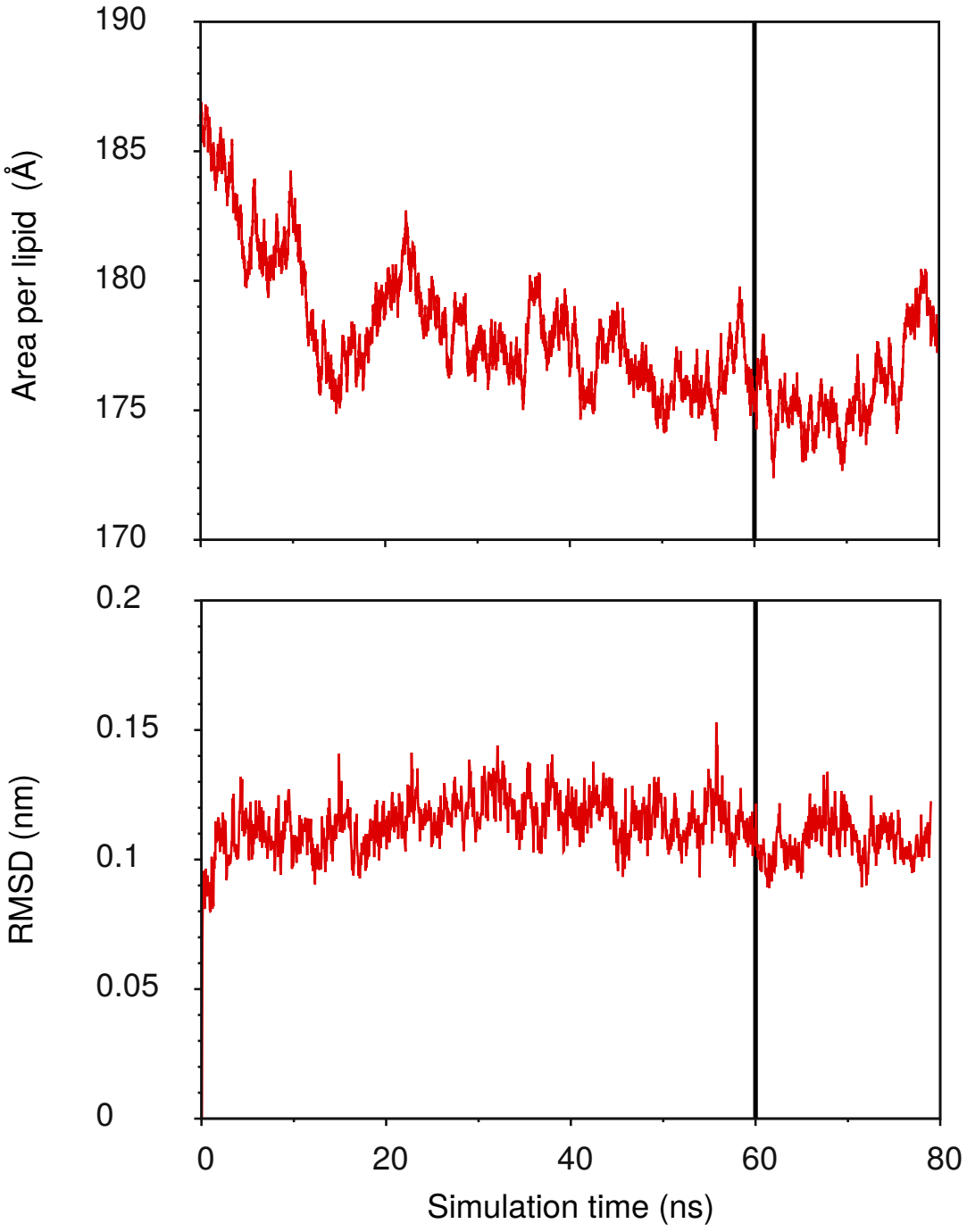

Figure S5: Upper panel: Area per lipid (area of the box simulation divided by the number of lipid molecules) for the whole restraint-free MD. Lower panel: RMSD for the backbone of CP29 for the whole restraint-free MD simulation. The vertical black line indicates the window from which we extracted the snapshots for coupling calculations.

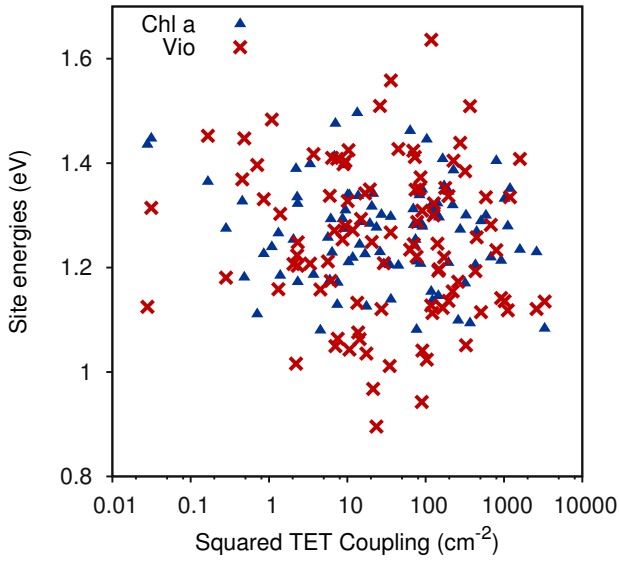

Figure S6: Scatter plot of the site energies of Violaxanthin (crosses) and Chl a603 (triangles) versus their squared TET coupling (logarithmic scale). R-squared values are 0.01 and 0.003, respectively. The site energies of Violaxanthin and Chl a603 are uncorrelated ($R^2 = 0.03$)

Table S2: Reorganization energies λ for the pairs considered in this work. The reorganization energies were computed from the variance of the energy gap along the MD trajectory, $\lambda = \sigma(\Delta E)^2/(2k_BT)$.

Pair		λ (cm^{-1})
Lut	a610	4620
	a612	5580
	a613	4850
Vio	a602	5020
	a603	5280
	a604	4380

References

(1) Ogata, K.; Yuki, T.; Hatakeyama, M.; Uchida, W.; Nakamura, S. *J. Am. Chem. Soc.* **2013**, *135*, 15670–3.

(2) Hornak, V.; Abel, R.; Okur, A.; Strockbine, B.; Roitberg, A.; Simmerling, C. *Proteins* **2006**, *65*, 712–725.

(3) Dickson, C. J.; Madej, B. D.; Skjevik, A. a.; Betz, R. M.; Teigen, K.; Gould, I. R.; Walker, R. C. *J. Chem. Theory Comput.* **2014**, *10*, 865–879.

(4) Zhang, L.; Silva, D.-A.; Yan, Y.; Huang, X. *J. Comput. Chem.* **2012**, *33*, 1969–80.

(5) Wang, J.; Wolf, R. M.; Caldwell, J. W.; Kollman, P. a.; Case, D. a. *J. Comput. Chem.* **2004**, *25*, 1157–74.

(6) Damjanović, A.; Ritz, T.; Schulten, K. *Biophys. J.* **2000**, *79*, 1695–705.

(7) You, Z.-Q.; Hsu, C.-P. *J. Phys. Chem. A* **2011**, *115*, 4092–100.

(8) Rondonuwu, F. S.; Taguchi, T.; Fujii, R.; Yokoyama, K.; Koyama, Y.; Watanabe, Y. *Chem. Phys. Lett.* **2004**, *384*, 364–371.

(9) Polívka, T.; Sundström, V. *Chem. Rev.* **2004**, *104*, 2021–71.

(10) Rondonuwu, F. S.; Watanabe, Y.; Fujii, R.; Koyama, Y. *Chem. Phys. Lett.* **2003**, *376*, 292–301.

(11) Hartzler, D. A.; Niedzwiedzki, D. M.; Bryant, D. A.; Blankenship, R. E.; Pushkar, Y.; Savikhin, S. *J. Phys. Chem. B* **2014**, *118*, 7221–32.